# Introduction

and-stage renal disease is commonly accompanied by the development of anemia caused by reduced production of the renal hormone erythropoietin, shortened erythrocyte life span caused by uremic toxins and oxidative stress, which are constant features of uremia. Common use of repeated blood transfusion to treat anemia was associated with a high incidence of iron overload in patients on dialysis (Vaziri, 2012).

A successful use of erythropoietic-stimulating agents (ESA) require sufficient available iron before and during therapy, almost all dialysis patients on ESA currently receive parenteral iron therapy. Transforming their quality of life and clinical outcomes. The dual risk of iron deficiency and iron overload must therefore be closely monitored in dialysis patients (Guy et al., 2016).

Recent Magnetic Resonance Imaging (MRI) studies have shown that most maintenance hemodialysis patients receiving intravenous (IV) iron supplementation have moderate to severe hepatic iron overload, considered a reason for concern (Carrilho et al., 2017).

The majority of CKD patients have liver iron overload before initiation of maintenance hemodialysis and that LIC increases steeply during the first year in dialysis with current anemia treatment. The findings strengthen the view that iron administration to CKD patients should be done with caution (Carrilho et al., 2017).



Ferritin levels alone are not fully acceptable and has poor specificity because It is an acute phase reactant, they may display considerable variations due to inflammation, infection, or any other chronic disorders. Moreover, there have been instances of heavy iron deposition, where the serum ferritin levels were disproportionately low (Fahmy et al., 2015).

In systemic iron overload, up to 70% to 90% of total body iron stores are found primarily in hepatocytes and Kupffer cells, mainly as ferritin and hemosiderin iron. Hepatic MRI has now emerged as the gold-standard method for estimating and monitoring iron stores in genetic hemochromatosis and secondary hemosiderosis (Rostoker et al., 2015).

Because liver biopsy is an invasive procedure that should be restricted to management of liver disease, attempts have been made to use imaging to detect and quantify hepatic iron content. However, iron deposition is not detectable at ultrasound examination, hyperdensity on CT scan is not specific for iron and can be masked by associated steatosis (Gandon et al., 2004).

MRI has been proposed for a rapid, non-invasive and cost effective technique that could limit use of liver biopsy for assessment, detection and quantification of liver iron content. We aimed to assess the accuracy of a simple, rapid, and easy to implement MRI procedure to detect and quantify hepatic iron stores (Gandon et al., 2004).

# AIM OF THE WORK

The aim of this study is to assess hepatic iron deposition among patients with ESRD on regular dialysis by using MRI T2\* relaxometry measures and correlating these values with serum ferritin.

#### Chapter 1

## MRI ANATOMY OF THE LIVER

he anatomy of the liver can be described by two different aspects: Morphological anatomy and Functional (segmental) anatomy. The morphological anatomy is based on the external appearance of the liver and does not show the internal structures as vessels and biliary ducts branching. The segmental anatomy of the liver is based on the vascular supply and drainage of the liver parenchyma. According to the classification of Couinaud and Bismuth whom are the first to divide the liver into eight functionally indepedent segments (*Charbel and Paul, 2016*).

#### Couinaud classification

- The Couinaud classification of the liver anatomy divides the liver into eight functionally indepedent segments. Each segment has separate vascular inflow, outflow and biliary drainage. In the centre of each segment there is a branch of portal vein, hepatic artery and bile duct. In the periphery of each segment there is vascular outflow through the hepatic veins (*Steve*, 2017).
  - o **Right hepatic vein** divides the right lobe into anterior and posterior segments.

- Middle hepatic vein divides the liver into right and left lobes (or right and left hemiliver). This plane runs from the inferior vena cava to the gallbladder fossa.
- The Falciform ligament divides the left lobe into a medial (segment IV) and a lateral part (segment II and III).
- The portal vein divides the liver into upper and lower segments. The left and right portal veins branch superiorly and inferiorly to project into the center of each segment (Steve, 2017).
- Normal frontal view of the liver show that segments VI and VII are not visible because they are located more posteriorly. The right border of the liver is formed by segment V and VIII. Although segment IV is a part of left hemiliver, it is situated more to the right. Couinaud divided the liver into a functional left and right liver by a main of portal scissurae containing the middle hepatic vein. This is known as cantlie's line (Fig.1). cantlie's line represent a line from the middle of the gallbladder fossa anteriorly to the inferior vena cava posteriorly (Steve, 2017).

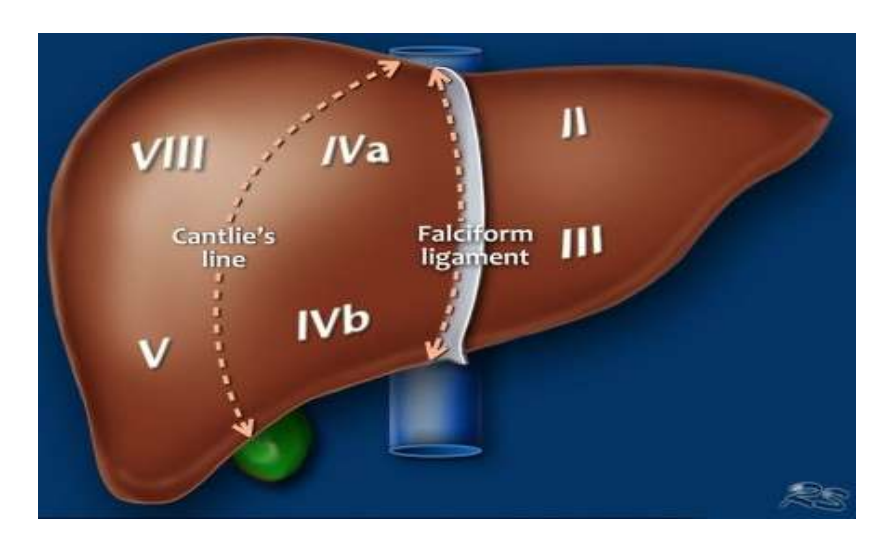
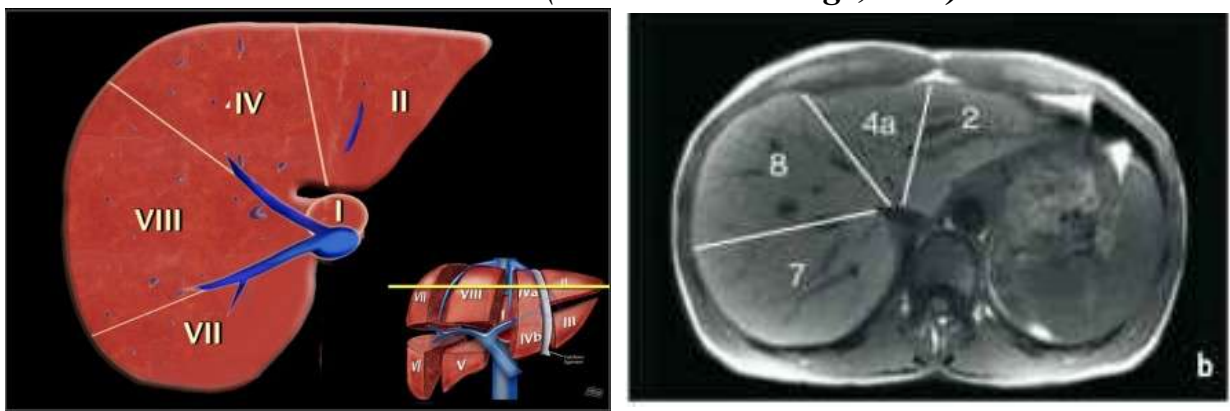


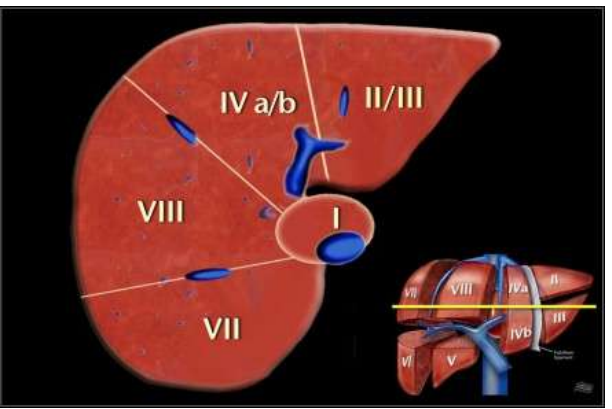
Fig. (1): Segmental anatomy of the liver

#### **Segments numbering**

■ There are eight liver segments (Figs.2,3,4,5), Segment IV is divided into segment IVa and IVb according to Bismuth. The numbering of the liver segments is in a clockwise manner. Segment I (the caudate lobe) is located posteriorly. So it is not visible on a frontal view (Smithuis and Lange, 2015).



**Fig. (2):** This figure is a transverse image through the superior liver segments, that are divided by the right and middle hepatic veins and the falciform ligament.



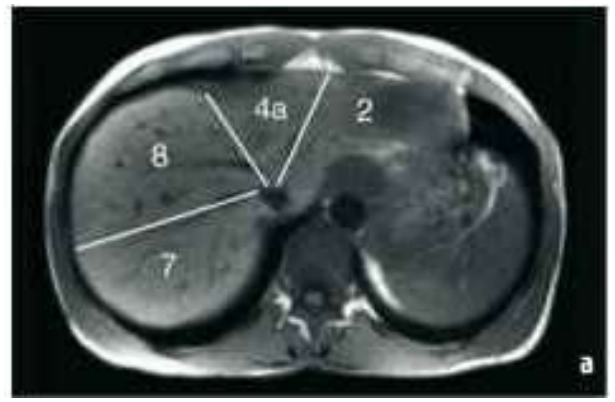
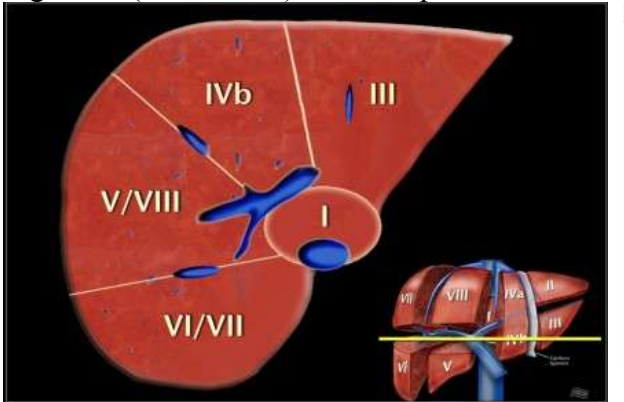
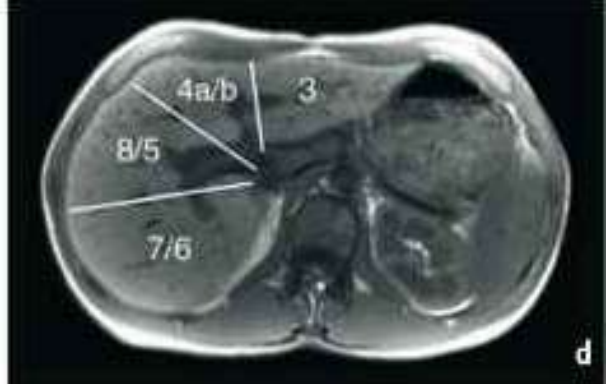
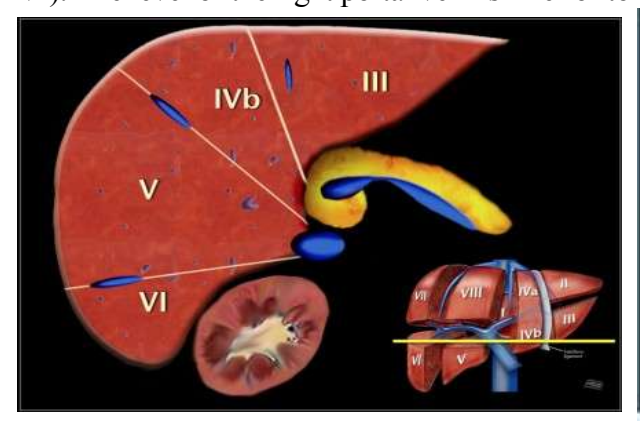


Fig. (3): This is a transverse image at the level of the left portal vein. At this level the left portal vein divides the left lobe into the superior segments (II and IVa) and the inferior segments (III and IVb). The left portal vein is at a higher level than the right portal vein.





**Fig. (4):** This image is at the level of the right portal vein. At this level the right portal vein divides the right lobe of the liver into superior segments (VII and VIII) and the inferior segments (V and VI). The level of the right portal vein is inferior to the level of the left portal vein.



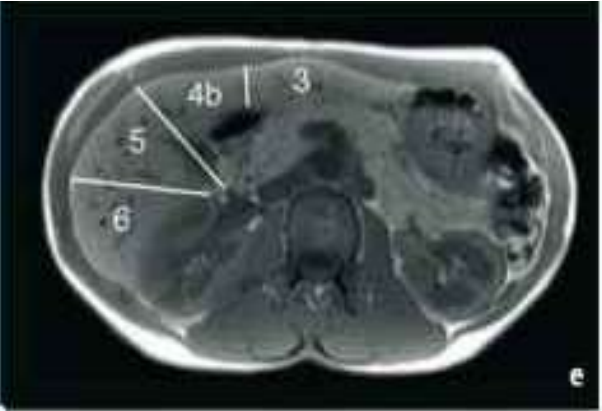


Fig. (5): At the level of the splenic vein, which is below the level of the right portal vein, only the inferior segments are visible (Smithuis and Lange, 2015).

**Table (1):** Description anatomic boundaries of each segment *(Charbel and Paul, 2016).* 

Segment	Vertical Boundary	Horizontal Boundary	Other
I	Middle of the IVC		Posterior to PV
П	Left of the left PV (falciform)	Cephalad to the left HV	
Ш	Left of the left PV (falciform)	Caudate to the left HV	
IVa	Right of the left PV (falciform) Left of the middle HV	Cephalad to the bifurcation of the PV	
IVЪ	Right of the left PV (falciform) Left of the middle HV	Caudate to the bifurcation of the PV	
V	Right of the middle HV Anterior to the right HV	Caudate to the bifurcation of the PV	
VI	Posterior to the right HV	Caudate to the bifurcation of the PV	
VII	Posterior to the right HV	Cephalad to the bifurcation of the PV	
VIII	Right of the middle HV Anterior to the right HV	Cephalad to the bifurcation of the PV	

#### How to separate liver segments on CT/MRI imaging?

- Left lobe: lateral(II/III) vs medial segment (IVA/B)
  Extrapolate a line along the falciform ligament superiorly
  to the confluence of the left and middle hepatic veins at
  the IVC (blue line).
- Left vs Right lobe: IVA/B vs V/VIII Extrapolate a line from the gallbladder fossa superiorly along the middle hepatic vein to the IVC (red line).
- Right lobe: anterior (V/VIII) vs posterior segment (VI/VII) Extrapolate a line along the right hepatic vein from the IVC inferiorly to the lateral liver margin (green line) (Fig.6) (Charbel and Paul, 2016).

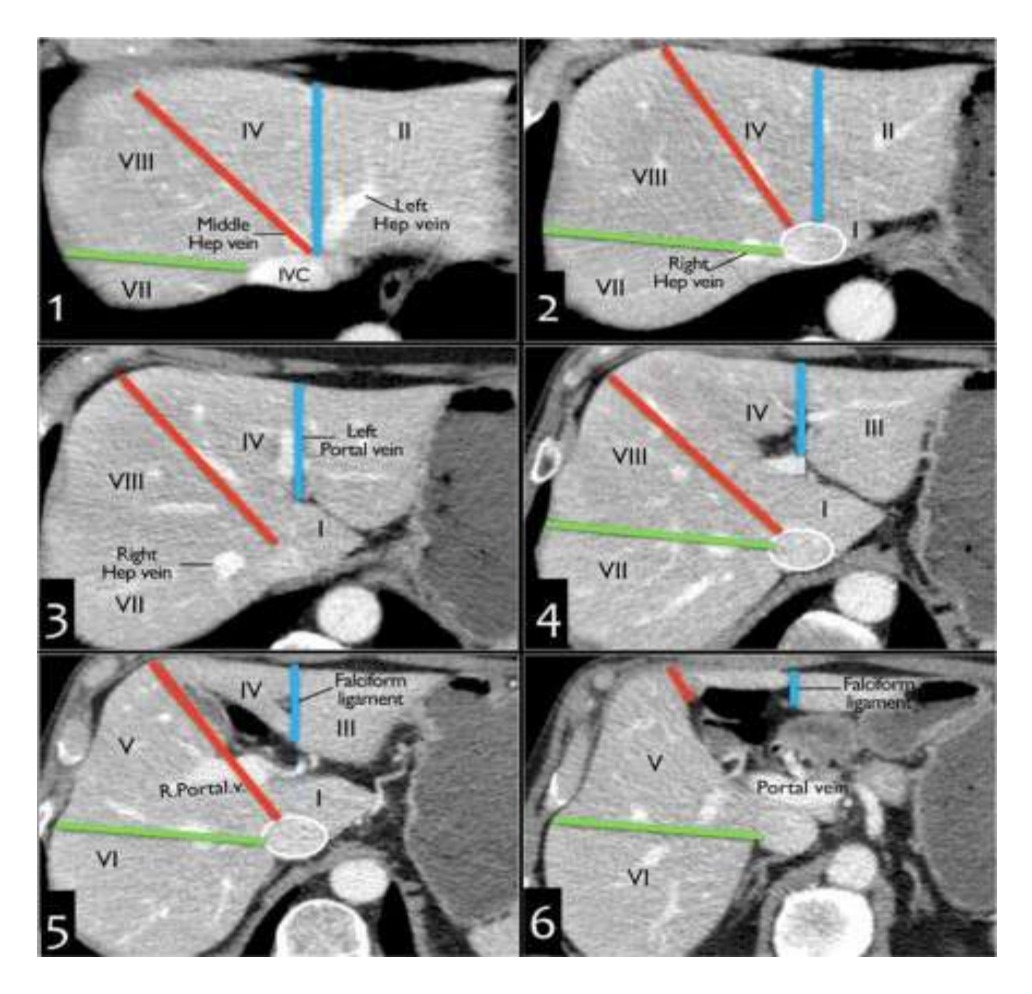


Fig. (6): Diagrammatic illustration of hepatic segments (Charbel and Paul, 2016).

The normal signal of the liver on T1WI is slightly hyperintense to muscle and kidneys. The signal was variable depending on the fat and iron content of the liver. In a fatty liver, the signal of the liver in T1WI is slightly hyperintense. While in a liver with high iron content, the signal on T1WI is slightly hypointense. The normal signal of the liver on T2WI is hypointense to the spleen, kidneys, and pancreas but slightly higher signal intensity than para-spinal muscles. The normal

signal of the liver on DWI is the same as on T2WI, the liver is hypointense to the kidneys and pancreas (Maniam and Szklaruk, 2010).

### Vascular supply of the Liver:

Liver has dual blood supply via portal vein and hepatic arteries.

#### • Portal vein:

The portal vein forms from the confluence of the splenic and superior mesenteric veins, and normally contributes a substantial portion of the hepatic blood flow (at least 75%). The main portal vein travels within the hepatoduodenal ligament as it enters the liver hilum. The portal vein typically bifurcates into right and left branches, each of which subsequently branches into anterior and posterior branches (right portal vein) or medial and lateral branches (left portal vein) (Figs. 7,8). These major branches further bifurcate to supply their respective hepatic segments. The portal vein branch to the caudate lobe can originate from either the left or the right portal vein (John, 2016).

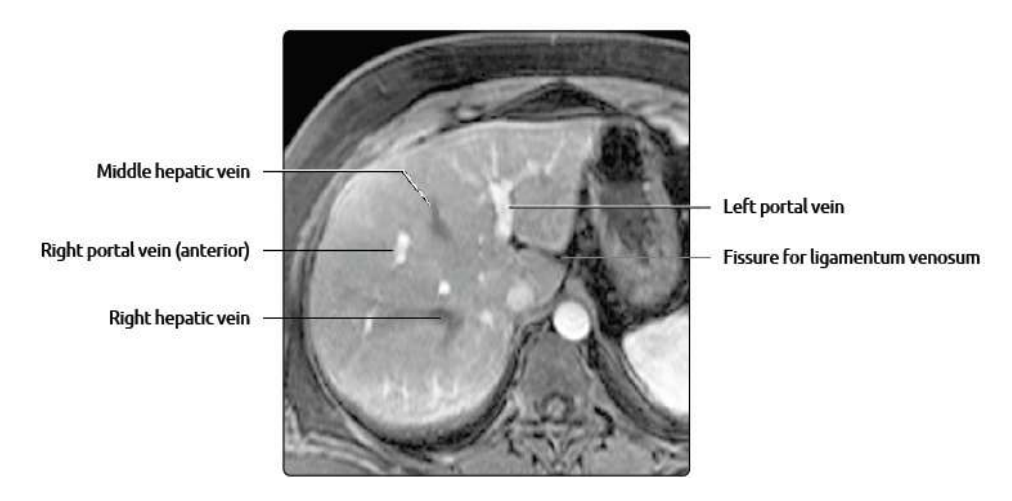


Fig. (7): MRI T1 post contrast demonstrate the left portal vein (Federle et al., 2017).



Fig. (8): MRI T1 post contrast shows the Right portal vein (Federle et al., 2017).

### • Hepatic artery:

The hepatic artery travels in the hepatoduodenal ligament anterior to the portal vein and supplies the liver with oxygenrich arterial blood and approximately 25% of the total hepatic blood flow. The common hepatic artery typically originates from the celiac axis together with the splenic and left gastric arteries (Fig.9). After giving of the gastroduodenal artery, the proper hepatic artery bifurcates into the right and left hepatic arteries, which further branch to supply the hepatic segments. The caudate lobe can receive its blood supply from branches of either the right or left hepatic artery (*John*, 2016).

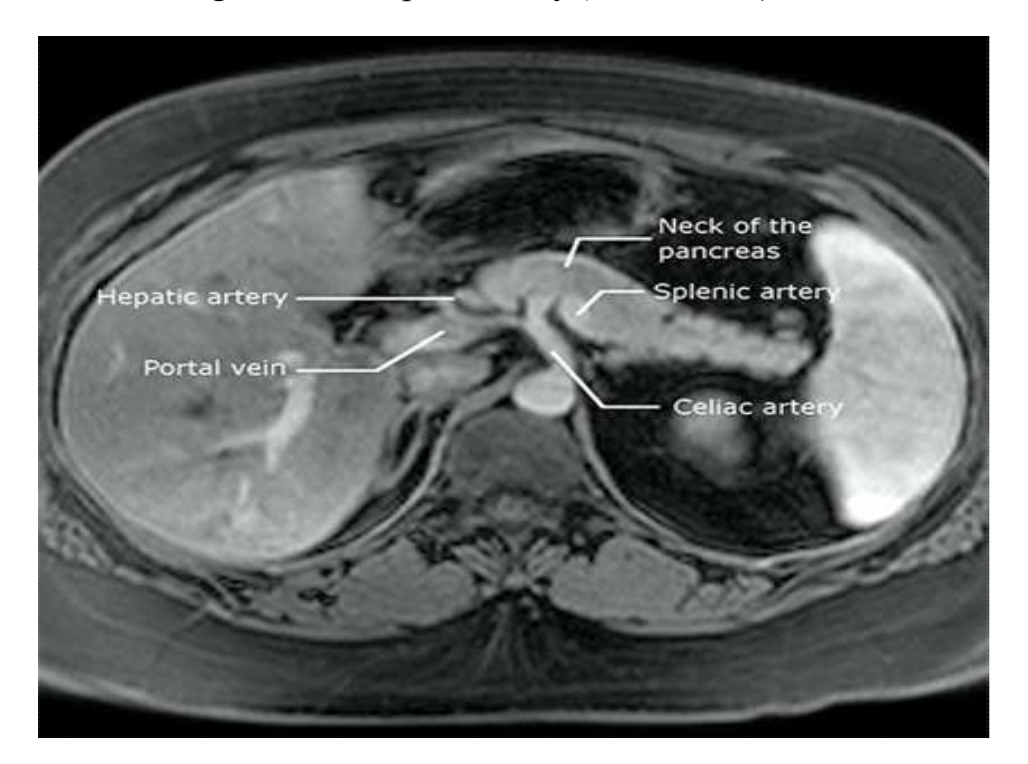


Fig. (9): MRI T1 Fat Sat post contrast. The hepatic artery arises from the celiac artery (*John*, 2016).

#### • Hepatic veins:

The right, middle, and left hepatic veins converge at the hepatic venous confluence and drain blood from the liver into the IVC just below the right atrium. The hepatic venous

confluence has a variety of configurations, but most commonly, the middle and left hepatic veins share a common trunk before entering the IVC (Fig.10). Segment I (caudate lobe) has a separate venous drainage directly to the IVC. Many individuals have accessory hepatic veins that drain the inferior right hepatic lobe directly into the IVC (*John*, 2016).

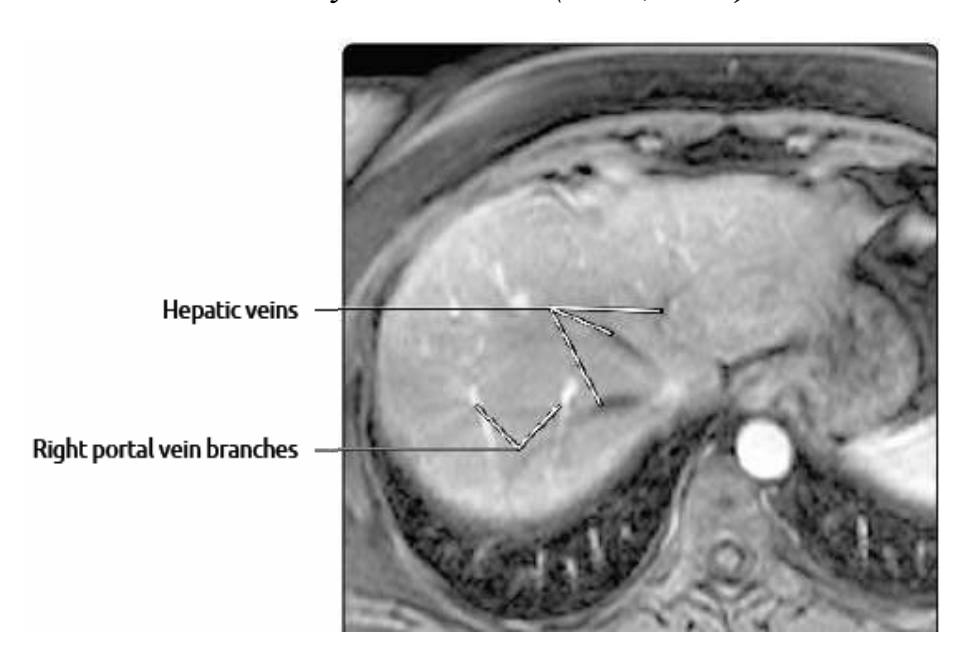
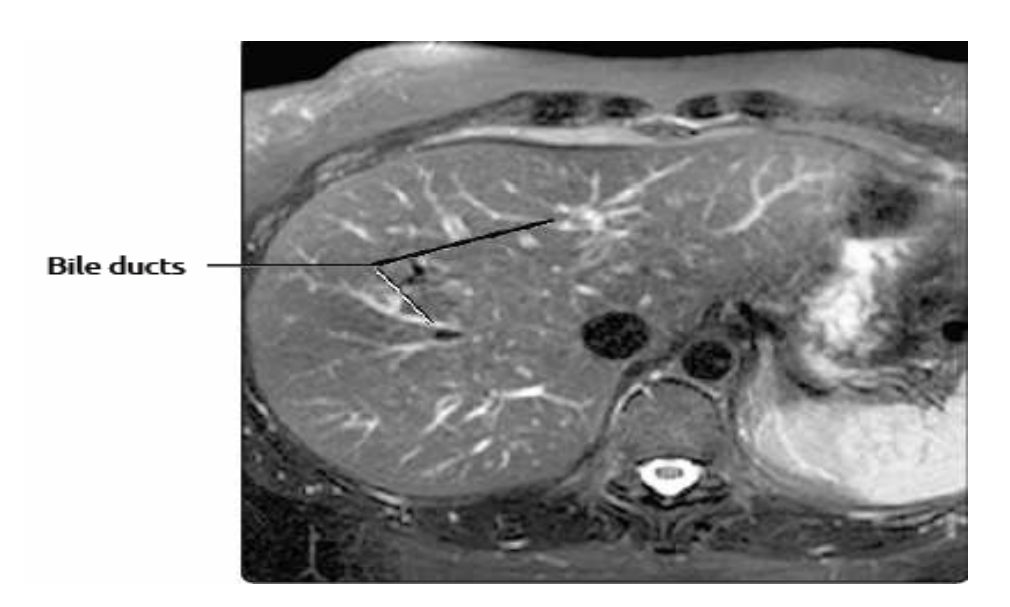


Fig. (10): Axial T1 post Gd shows the confluence of the hepatic veins (Federle et al., 2017).

#### • Portal triad:

At all levels of size and subdivision, branches of hepatic artery, portal vein, and bile ducts travel together. Blood flows into hepatic sinusoids from interlobular branches of hepatic artery and portal vein  $\rightarrow$  hepatocytes (detoxify blood and produce bile)  $\rightarrow$  bile enters bile ducts and blood enters central veins  $\rightarrow$  hepatic veins (*Federle et al., 2017*).



**Fig. (11):** Axial T2 weighted fat suppressed MR images shows relatively low signal from the liver parenchyma. Flowing blood appears very dark, while static fluid, such as bile and spinal fluid, appears quite bright. The branching pattern of the intrahepatic bile ducts is evident. A more central location shows the bile ducts becoming larger as they approach the porta hepatis *(Federle et al., 2017)*.

### Chapter 2

# PATHOPHYSIOLOGY AND THE MECHANISM OF HEPATIC IRON DEPOSITION

he human body has no mechanism for excreting excess iron, which is stored as crystalline iron oxide within ferritin and haemosiderin in the body. Transfusional iron leads to iron deposition in the reticulo-endothelial system of the spleen, liver and bone marrow. In advanced cases iron also accumulates in parenchymal cells of the liver, heart, pancreas and endocrine organs, which are sensitive to the toxic effects of iron. When the iron-binding capacity of transferrin is exhausted, free iron appears as non-transferrin bound iron (NTBI). The toxicity of NTBI is much higher than bound iron and promotes hydroxyl radical formation resulting in peroxidative damage to membrane lipids and proteins (Anderson et al., 2001).

The liver is the dominant storage organ for excess iron and readily acquires excess transferrin and non-transferrin bound iron, it also mobilizes iron rapidly and efficiently in times of demand or in response to iron chelation, Even then cardiac iron uptake is delayed compared to many other extrahepatic organs including the pancreas. Thus many young patients can exhibit severe hepatic iron overloading with no evidence of cardiac iron overloading (Wood et al., 2008).